Reconciling the light component and all-particle cosmic ray energy spectra at the knee[*]

ZHAO Yi(赵熠)[1,2;1]   JIA Huan-Yu(贾焕玉)[1;2]   ZHU Feng-Rong(祝凤荣)[1]

[1] Southwest Jiaotong University, Chengdu 610031, China

[2] Key Laboratory of Particle Astrophysics, Institute of High Energy Physics, Chinese Academy of Science, Beijing 100049, China

Abstract: The knee phenomenon of the cosmic ray spectrum, which plays an important role in studying the acceleration mechanism of cosmic rays, is still an unsolved mystery. We try to reconcile the knee spectra measured by ARGO-YBJ and Tibet-III. A simple broken power-law model fails to explain the experimental data. Therefore a modified broken power-law model with non-linear acceleration effects is adopted, which can describe the sharp knee structure. This model predicts that heavy elements dominate at the knee.

Key words: energy spectrum, knee, composition

1   Introduction

The energy spectrum of cosmic rays, an important key to realize the origin and acceleration mechanism of cosmic rays, can be simply described by a power law over many magnitudes of energy from 10^9 eV to 10^{20} eV [1], except for a few distinctive structures, such as the knee phenomenon around 4×10^{15} eV. The spectral power index rapidly steepens from about -2.7 before the knee to -3.1 over the knee [2]. Numerous works on cosmic ray propagation and acceleration mechanisms [1, 3–10] have been done to investigate the origin of the knee. These include the diffusive shock acceleration (DSA) spectra origin of the knee based on the theory of non-linear diffusive particle acceleration by shock waves from supernova remnants (SNRs) [11, 12], and the contribution of nearby pulsar wind producing very hard spectra in the power-law spectra in the knee region [13, 14]. However, the origin of the knee structure is still unconfirmed. Currently, the interpretations of this phenomenon are based on phenomenological models from experimental measurements. Many results have been given by direct observations with balloon detectors [15–17] and indirect observations with air-shower detectors on high altitude mountains [18–20]. The CREAM experiment, as a balloon detector, has announced precise measurements of energy spectra for individual nuclei ranging from 2 TeV to 200 TeV [21]. As an air-shower ground-based detector located 4300 m above sea level, the Tibet-III array has presented an all-particle energy spectrum of primary cosmic rays from 100 TeV to

100 PeV, revealing a sharp knee structure around 4 PeV. Another air-shower experiment with the same altitude as Tibet-III, ARGO-YBJ, recently gave a new measurement of the energy spectrum of hydrogen and helium nuclei, exhibiting a clear knee structure [22].

The latest measurements released by ARGO-YBJ are investigated by the joint operation of Resistive Plate Chambers (RPC) detectors and a Cherenkov telescope. This hybrid detection bridges the gap between balloon detectors and ground-based experiments, improves the shower energy resolution and enhances the capability to discriminate showers induced by light nuclei from events initiated by heavier nuclei. They yield clear evidence for a knee-like structure in the spectrum of hydrogen and helium nuclei under 1 PeV [22].

In the following discussions, we explain the knee spectra measured by ARGO-YBJ and Tibet-III by phenomenological models. The superposition of energy spectrum of individual components described by a simple broken power-law cannot reconcile the light components and all-particle energy spectra. We therefore propose a parametric model to reconcile them. In Section 2 we give two different scenarios and parameters to fit the experimental data. Section 3 presents the average mass. Finally, Section 4 gives some discussion and conclusions.

2   Energy spectra formulation

Cosmic rays emitted from the sources are most likely

accelerated in the strong shock fronts of SNRs by the DSA mechanism. The particles are deflected by chaotic magnetic fields, cross shock fronts frequently, and therefore gain energy up to the PeV region. This acceleration leads to the observed approximate power-law spectrum. The energy spectrum is modified during diffusive propagation. The spectra near the sources vary from that observed on the earth, which may be due to nuclear spallation or decay, ionization losses, leakage from the galaxy and solar modulation for low energies [23–25]. We try to adopt two different phenomenological models to explain the observed energy spectra around knee structure. One is an expression of a simple broken power-law and the other is the broken power-law with non-linear modification term.

2.1   Broken power-law model and parameters

The all-particle primary energy spectra derived from extensive air shower experiments can be described by a broken power-law function. We therefore use this kind of function to parameterize the observed differential energy spectra for individual elements of cosmic ray, which can be written as

$$\frac{\mathrm{d}j}{\mathrm{d}E}=j_0 E^{-\gamma}\left(1+\frac{E}{z\epsilon_{\mathrm{b}}}\right)^{-\Delta\gamma}, \qquad (1)$$

where $\frac{\mathrm{d}j}{\mathrm{d}E}$ is the differential flux of the individual element with energy E, j_0 is the normalization constant, ϵ_b represents the break point of the proton spectrum, z is the atomic number, γ is the power index in the energy range $E\ll z\epsilon_{\mathrm{b}}$, and $\gamma+\Delta\gamma$ denotes the power index when $E\gg z\epsilon_{\mathrm{b}}$. We try to use this expression to fit both the combined energy spectrum of hydrogen and helium nuclei observed by ARGO-YBJ and the all-particle energy spectrum given by Tibet-III. The interaction model SIBYLL for Tibet data is used in this work. We firstly fix the energy spectra of each component below the knee region, and then extrapolate the spectra beyond the knee. The observed data of individual elements (H, He, C, O, Ne, Mg, Si and Fe) from CREAM are adopted. For the spectrum index of each element, see [21, 26]. An expression of simple power-law $\mathrm{d}j/\mathrm{d}E=jE^{-\gamma}$ is used to fit the spectrum of each component, with the fitting parameters j and spectral indices listed in Table 1.

With Eq. (1), we fit the combined spectrum of hydrogen and helium nuclei observed by ARGO-YBJ [18, 22, 27], and get the fitting result of energy break point $\epsilon_{\mathrm{b}}=4\times10^{14}$ eV and $\Delta\gamma=0.68$ for the proton. The break point for other elements can be calculated by $z\epsilon_{\mathrm{b}}$. The spectral indices of all elements at the higher energy range beyond the knee region are assumed to be the same value as the result from ARGO-YBJ, i.e. $-\gamma-\Delta\gamma=-3.34$. We sum up the energy spectra of all elements to get the approximate all-particle spectrum, seen as the red solid

line in Fig. 1. It can be seen from Fig. 1 that this all-particle spectrum based on ARGO-YBJ observation with this simple broken power-law model cannot match the observed all-particle spectrum given by Tibet-III. The simple broken power-law function therefore cannot describe the energy spectrum in the knee region, which perhaps is due to the influence of the DSA mechanism.

Table 1.   Constant j and spectrum index γ below the knee region.

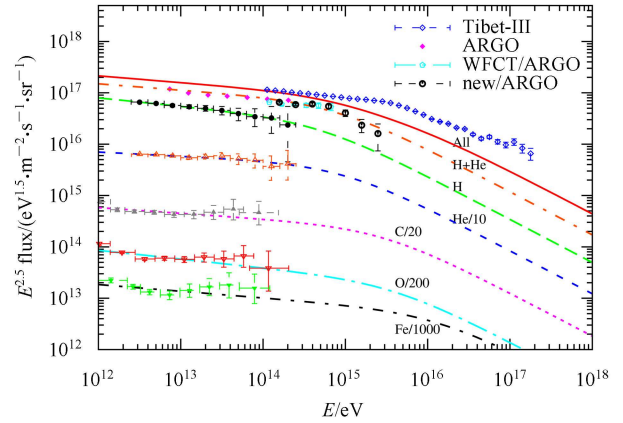| z	element	$j/(\mathrm{eV}^{-1}\cdot\mathrm{m}^{-2}\cdot\mathrm{s}^{-1}\cdot\mathrm{sr}^{-1})$	γ
1	H	6.62×10^{18}	2.66
2	He	6.40×10^{17}	2.58
6	C	2.43×10^{17}	2.61
8	O	1.88×10^{18}	2.67
10	Ne	1.68×10^{18}	2.72
12	Mg	4.56×10^{17}	2.66
14	Si	7.99×10^{17}	2.67
26	Fe	6.71×10^{17}	2.63

Fig. 1.   (color online) All-particle spectrum (red solid line) calculated as the sum of individual components, with spectra of some individual elements. The data are cited from CREAM [21, 26], ARGO-YBJ [18, 22, 27] and Tibet-III [19].

2.2   Non-linear model and parameters

Since the differential energy spectrum in the form of the simple broken power-law cannot reconcile the observations of ARGO-YBJ and Tibet-III, a new correction term is added, so the broken power-law can now be expressed as

$$\frac{\mathrm{d}j}{\mathrm{d}E}=j_0 E^{-\gamma}\left[1+\alpha\left(\frac{E}{z\epsilon_{\mathrm{b}}}\right)^{\beta}\right]\left(1+\frac{E}{z\epsilon_{\mathrm{b}}}\right)^{-\Delta\gamma}, \qquad (2)$$

where α is assumed to be a z-dependent parameter, and β is a constant. The DSA mechanism may result in a spectrum with concave-up curvature, so we multiply the non-linear term $1+\alpha\left(\dfrac{E}{z\epsilon_{\mathrm{b}}}\right)^{\beta}$ into the simple broken power-law to structure a concave-up form as a phenomenological model. Without this non-linear term, the

superimposed all-particle spectrum from all elements is smooth and cannot fit the sharp knee structure as measured by Tibet-III. In addition, we have tried some parameters in a non-z-dependent form, but these cannot match the data, so we finally adopt the form in Eq. (2). An equation to express the non-linear effects is proposed in [28]. They propose the non-linear process by a modified exponential cut-off expression for the spectra from sources, and then deduce the observed spectra by the superposition of these spectra. From their formula, the model they deduced is a kind of broken power-law multiplied by a complex modified term. While our expression form is simpler, we modify the simple broken power-law directly as the observed spectra and then parameterize this scenario. Combined with the newly published measurements from ARGO-YBJ, our model is easier to quantify the parameters precisely. A model with precisely confirmed parameters will help us to review its intrinsic physical issues. From Eq. (2), we get a good fit result to match the observations from both ARGO-YBJ and Tibet-III with parameters $\alpha=1.50+0.35z$, $\beta=1.20$,

$\epsilon_{\mathrm{b}}=2.0\times10^{14}$ eV and $\Delta\gamma=1.88$ for the proton. $\Delta\gamma$ values of other elements are assumed to obey the formula $-\gamma-\Delta\gamma+\beta=-3.34$. The fitting spectra are plotted in
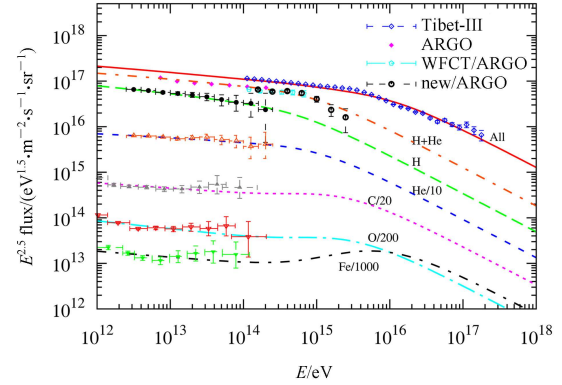

Fig. 2. (color online) All-particle spectrum (solid red line) calculated as the sum of individual components, with spectra of some individual elements. The data are cited from CREAM [21, 26], ARGO-YBJ [18, 22, 27] and Tibet-III [19].
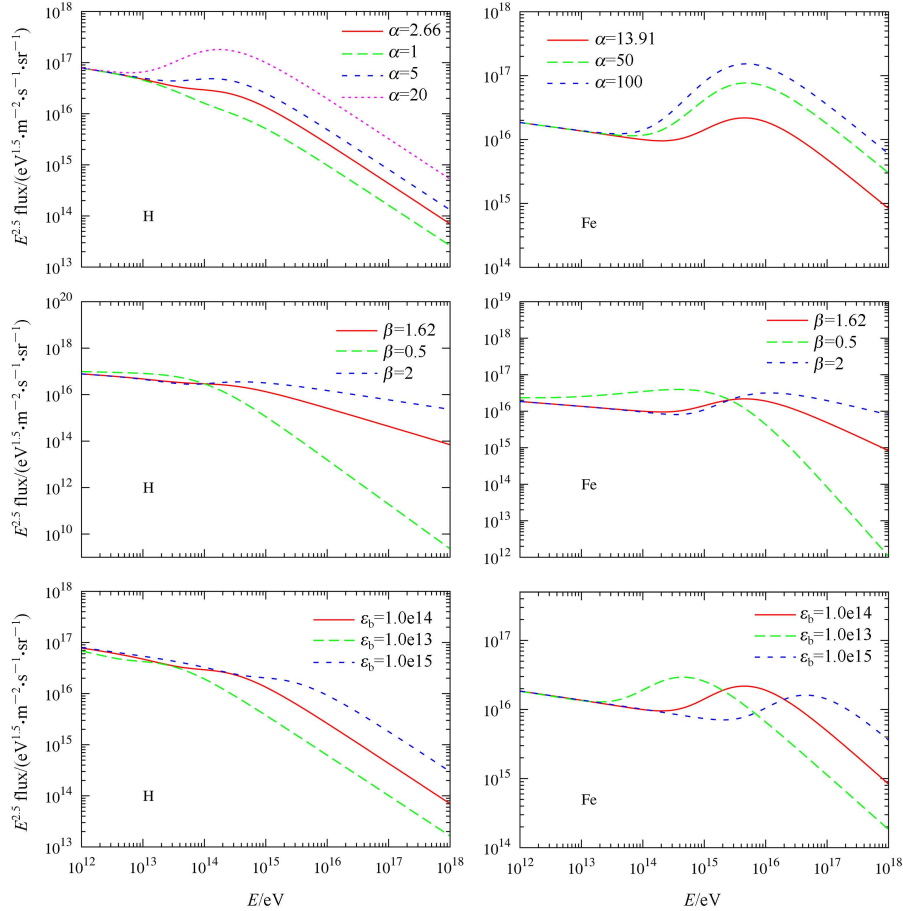

Fig. 3. (color online) Energy spectrum shapes determined by α, β and ϵ_{b} for elements H (left) and Fe (right). The upper two figures represent the dependence of the spectra on α, the middle two figures represent the dependence on β, and the lower two figures represent the dependence on ϵ_{b}. The solid red lines in all six figures represent the currently used values.

Fig. 2, where the solid red line represents the all-particle spectrum. From Fig. 2 we can see that the all-particle spectrum based on ARGO-YBJ observation can match the observed all-particle spectrum given by Tibet-III. Based on this model, the distinctive knee structure is mostly contributed by heavy elements such as Fe.

In order to obtain the best fitting parameters for the non-linear model, we employ the Markov Chain Monte Carlo (MCMC) [29, 30], a very efficient algorithm, to achieve our goal. Considering that the calculation of χ^2 will be affected by the too small errors of all-particle spectrum given by Tibet-III, we amplify the errors of this spectrum by taking account of energy resolution. The initial form of data with errors listed in the literature [19] are expressed by $F\pm\Delta F$, where F denotes the flux and ΔF denotes the systematic error. As a new deduced additional error, a new term is added to this expression, i.e. $F\pm\Delta F\pm F(\gamma-1)(\Delta E/E)$, where γ denotes the spectrum index. We take the energy resolution $\Delta E/E=0.15$ as a constant. The following 5 parameters: $\alpha=p_1+p_2z$, β, $\epsilon_{\rm b}$ and $\Delta\gamma$, are set free for the MCMC algorithm, where α consists of free parameters p_1, p_2 and redshift z. The parameters $\epsilon_{\rm b}$ and $\Delta\gamma$ here refer to protons as mentioned above. Because every spectrum index of elements in the higher energy band beyond the knee is supposed to be the same value, we can get the $\Delta\gamma$ of other components from the $\Delta\gamma$ of the proton. By this MCMC algorithm, we obtain the best fitting parameters as follows: $\alpha=2.21+0.45z$, $\beta=1.62$, $\epsilon_{\rm b}=1.0\times10^{14}$ eV and $\Delta\gamma=2.25$ for the proton. The parameters α, β and $\epsilon_{\rm b}$ decide the shapes of the energy spectra. Different values result in different spectra, as shown in Fig. 3, where the elements H and Fe are taken as examples.

The best fit result is shown in Fig. 4. The measurements of hydrogen and helium nuclei spectra using the SIBYLL model by the KASCADE group [31] are compared with our model in Fig. 4. The KASKADE group claimed that the energy spectra of both proton and helium show a knee-like feature, but in our model, this seems not to be the case.

3   Average mass

A commonly-used quantity to characterize the mass composition of cosmic rays is the mean logarithmic mass, which is defined as

$$\langle \ln A \rangle = \sum_i r_i \ln A_i, \qquad (3)$$

r_i being the relative fraction of nuclei of mass A_i. The average mass is reported by many air shower experiments, but the results are divergent because of the poor primary mass resolution. We calculate the average mass for two cases: one for the former non-linear model and another for the latter best fitting case, as shown in Fig. 5.
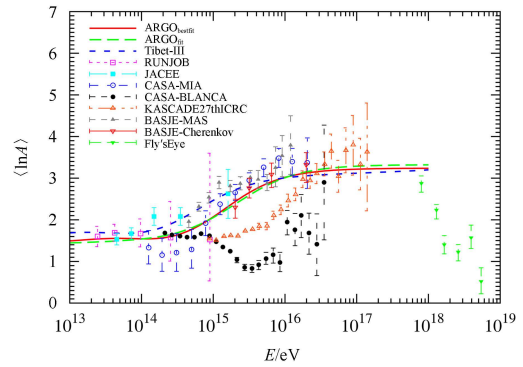
Fig. 5.   (color online) Average mass calculated for the non-linear model, compared with that of Tibet-III (blue dashed line). The green dashed line represents the first fitting result by the non-linear model and the red solid line represents the best fitting result. The data are cited from RUNJOB [32], JACEE [33], CASA/MIA [34], CASA/BLANCA [35], KASCADE 27thICRC [36], BASJE-MAS and BASJE-Cherenkov [20], and Fly's Eye [37].

From our derived average mass of cosmic rays, we can see $\langle \ln A \rangle$ goes up between several hundreds of TeV and several tens of PeV. It implies that heavier components occupy an increasing proportion with the increase of energy, and predicts an iron-dominant composition above the knee. But the components above the knee are not all Fe, because $\langle \ln A \rangle$ for Fe is about 4.0. Further experimental measurements of the chemical composition of high energy cosmic rays will verify our prediction. If the light components dominate the knee structure, this model can be excluded, while if the heavy components dominate the knee structure, this model will be confirmed, and the measurements will be helpful to improve the model parameters.
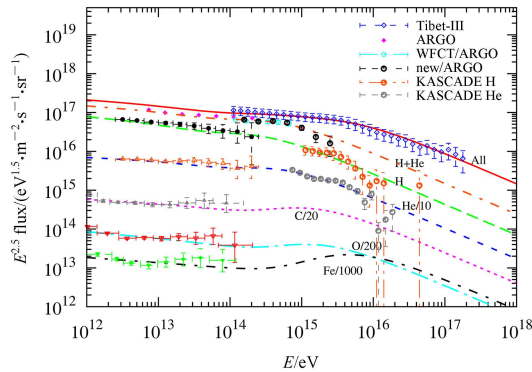
Fig. 4.   (color online) All-particle spectrum (solid red line) calculated as the sum of individual components, with spectra of some individual elements. The data are cited from CREAM [21, 26], ARGO-YBJ [18, 22, 27], Tibet-III [19] and KASCADE [31].

4   Discussion and conclusion

Many mechanisms have been discussed to explain the knee structure of cosmic rays, including the diffusive shock acceleration mechanism of cosmic rays in supernova explosion shock fronts, leakage from the galaxy, interactions with background particles in the interstellar medium, and new physics of interactions in the atmosphere. Some models are likely to be excluded, however, such as the leaky box model, interactions with background particles and new types of interactions in the atmosphere. The leakage from the galaxy does not give a distinct change of the spectral slope at the knee. The scenario of interactions with background particles yields a very light mean logarithmic mass, while the measurements indicate an increase of mass with energy. For new types of interactions in the atmosphere, there are no inconsistencies between the different air shower components by the simultaneous observations from KASCADE, and the measurements of different air shower components can be interpreted with standard particle physics [38].

We propose two scenarios to reconcile the light components and all-particle energy spectra by phenomenological models. In the first scenario, we use a simple broken power-law model to fit the combined energy spectrum of hydrogen and helium nuclei measured by ARGO-YBJ and the all-particle spectrum measured by Tibet-III, but the all-particle spectrum cannot be fitted by this model. Hence, the simple broken power-law fails to explain the knee structure. In the second scenario, a non-linear modification term is added to the broken power-law. This modified broken power-law model with non-linear acceleration effects can describe the sharp knee structure. The mechanism of non-linear effects at shock fronts of SNRs has been explained in earlier works [39]. Particles with higher energies can scatter farther ahead of the shock, which results in an effectively higher compression ratio, so a more locally hard spectrum is produced, and a concave-up curvature to the accelerated-particle distribution is expected [40]. In addition, this modified model predicts that heavy elements dominate at the knee. Based on this model, some models holding the viewpoints of weak knee structure or protons dominating the knee are likely to be excluded. Precise measurements of energy spectra of individual elements in the knee region will test our model.

References

1 Blümer J, Engel R, Hörandel J R. Prog. Part. Nucl. Phys., 2009, **63**: 293
2 Kulikov G V, Khristiansen G B. J. Exp. Theor. Phys., 1958, **35**: 635
3 Ptuskin V S, Rogovaya S I, Zirakashvili V N et al. Astron. Astrophys., 1993, **268**: 726
4 Candia J, Roulet E, Epele L N. J. High Energy Phys., 2002, **12**: 33
5 Berezhko E G, Ksenofontov L T. J. Exp. Theor. Phys., 1999, **89**: 391
6 Stanev T, Biermann P L, Gaisser T K. Astron. Astrophys., 1993, **274**: 902
7 Jokipii J R. Astrophys. J., 1982, **255**: 716
8 Jokipii J R. Astrophys. J., 1987, **313**: 842
9 Kobayakawa K, Honda Y S, Samura T. Phys. Rev. D, 2002, **66**: 083004
10 Völk H J, Zirakashvili V N. Astron. Astrophys., 2004, **417**: 807
11 Hillas A M. J. Phys. G, 2005, **31**: 95
12 Gaisser T K. Astropart. Phys., 2012, **35**: 801
13 Bhadra A. Proc. Int. Cosmic Ray Conf., 2005, **3**: 117
14 Erlykin A, Martirosov R, Wolfendale A. CERN Courier, 2011, **51**(1): 21
15 Wefel J P, Adams J H, Ahn H S et al. Proc. Int. Cosmic Ray Conf., 2005, **3**: 105
16 Seo E S, Ahn H S, Allison P et al. Proc. Int. Cosmic Ray Conf., 2005, **3**: 101
17 Ave M, Boyle P J, Gahbauer F et al. Astrophys. J., 2008, **678**: 262
18 Bartoli B, Bernardini P, BI X J et al. Chin. Phys. C, 2014, **38**: 045001
19 Amenomori M, BI X J, CHEN D et al. Astrophys. J. , 2008, **678**: 1165
20 Ogio S, Kakimoto F, Kurashina Y et al. Astrophys. J., 2004, **612**: 268
21 Yoon Y S, Ahn H S, Allison P S et al. Astrophys. J., 2011, **728**: 122
22 Bartoli B, Bernardini P, BI X J et al. arXiv:astro-ph.HE/1502.03164
23 Blandford R, Eichler D. Phys. Rept., 1987, **154**: 1
24 Cesarsky C J. Annu. Rev. Astron. Astrophys., 1980, **18**: 289
25 Letaw J R, Silberberg R, Tsao C H. Astrophys. J., 1993, **414**: 601
26 Ahn H S, Allison P, Bagliesi M G et al. Astrophys. J., 2009, **707**: 593
27 Bartoli B, Bernardini P, BI X J et al. Phys. Rev. D, 2012, **85**: 092005
28 Shibata M, Katayose Y, HUANG J et al. Astrophys. J., 2010, **716**: 1076
29 Lewis A, Bridle S. Phys. Rev. D, 2002, **66**: 103511
30 LIU J, YUAN Q, BI X J et al. Phys. Rev. D, 2012, **85**: 043507
31 Antoni T, Apel W D, Badea A F et al. Astropart. Phys., 2005, **24**: 1
32 Apanasenko A V, Sukhadolskaya V A, Derbina V A et al. Astropart. Phys., 2001, **16**: 13
33 Asakimori K, Burnett T H, Cherry M L et al. Astrophys. J. , 1998, **502**: 278
34 Glasmacher M A K, Catanese M A, Chantell M C et al. Astropart. Phys., 1999, **10**: 291
35 Fowler J W, Fortson L F, JUI C C H et al. Astropart. Phys., 2001, **15**: 49
36 Hörandel J R. Proc. Int. Cosmic Ray Conf., 2001, **1**: 71
37 Bird D J, Corbató S C, DAI H Y et al. Phys. Rev. Lett., 1993, **71**: 3401
38 Hörandel J R. Astropart. Phys., 2004, **21**: 241
39 Malkov M A, O'C Drury L. Rep. Prog. Phys., 2001, **64**: 429
40 Reynolds S P. Annu. Rev. Astron. Astrophys., 2008, **46**: 89